THE ANNALS OF "DUNAREA DE JOS" UNIVERSITY OF GALATI
FASCICLE III, 2008, Vol.31, No.1, ISSN 1221-454X
ELECTROTECHNICS, ELECTRONICS, AUTOMATIC CONTROL, INFORMATICS

# MPPT ALGORITHM FOR SMALL WIND SYSTEMS BASED ON SPEED CONTROL STRATEGY

**Ciprian VLAD, Emil CEANGA**

*"Dunărea de Jos" University of Galați, Electrical and Electronics Engineering Faculty, Stiinței, no. 2, 8000146 – Galați, Romania.*

Abstract: This paper presents experimental results of an autonomous low-power wind energy conversion system (WECS), based on a permanent-magnet synchronous generator (PMSG) connected directly to the wind turbine. The purpose of this paper is to present an improving method for MPPT (Maximum Power Point Tracking) algorithm based shaft rotational speed optimal control. The proposed method concern the variable delay compensation between measured wind speed from anemometer and wind shaft rotational speed proportional signal. Experimental results aiming to prove the efficiency of the proposed method are presented.

Keywords: wind system, permanent-magnet synchronous generator, maximum power point tracking.

## 1. INTRODUCTION

Variable-speed wind turbines are currently the most used WECS. The variable-speed operation is possible due to the power electronic converters interface. Full variable-speed WECS are very flexible in terms of which type of generator is used. It can be equipped with either an induction or a synchronous generator. Permanent-magnet synchronous generators are used more frequently in low-to-medium power WECS applications (Munteanu *et al.*, 2008).

The PMSG is considered, in many research articles, a good option to be used in WECS, due to its self-excitation property, which allows operation at high power factor and efficiency (Alatalo 1996).

Control plays an ever increasing role in modern WECS. There are numerous research articles dedicated to WECS control, all of them having starting from the idea that control can and does significantly improve all aspects of WECS (Burton *et al.,* 2001) .

For the fixed-pitch turbines operating in partial load, maximum energy capture available in the wind can be achieved if the turbine rotor operates on the optimal regime characteristic (ORC). This regime can be obtained by tracking some target variables: the optimal rotational speed, depending proportionally on the wind speed, the optimal rotor power, which depends proportionally on the rotational speed cubed or the optimal wind torque which is proportionally with the squared rotational speed (Munteanu *et al.*, 2008).

The shaft rotational speed optimal control approach using a set point from the wind speed information has some drawbacks related to the wind speed being measured by an anemometer mounted on the nacelle, which offers information on the fixed-point wind speed. This information differs from the wind speed experienced by the blade, mainly because of the time lag between the two signals. That's why, nowadays this solution is less used compared with power control one (when the reference depends of rotational speed). In speed closed loop control case the system's properties are simples, since in power control are sophisticated (with nonlinear evolutions)(Vlad, 2008).

The aim of this paper is to present a solution which uses a maximum power point tracking rotational speed close loop control for wind system performances improvement.

This paper was recommended for publication by Marian Gaiceanu

The paper is organized as follows. The next section describes the experimental rig used to carry-out the real-time tests. The third section presents the control solution used to maximize the wind power whereas the fourth section discusses the main results of MPPT algorithm based shaft rotational speed optimal control. The last section is dedicated to conclusions.

## 2. EXPERIMENTAL RIG

The experimental rig is composed of two subsystems:

1) The electromechanical subsystem;
2) The electrical, control and supervision subsystem.

The hardware/software support of the whole experimental rig is ensured by the dSPACE board DS 1103. The electromechanical wind turbine simulator is built based upon the hardware-in-the-loop simulation concept (Tan *et al.*, 2004). This simulator provides a "wind shaft" where the steady-state and dynamic characteristics of a given turbine can be replicated.

The simulator is composed of:

- A closed-loop servo-system, consisting of a Danfoss VLT 5005 Flux inverter, which controls an asynchronous motor with 960 rpm rated speed and 3 kW rated power. This means that wind turbines of 3 kW maximum rated power can be simulated;
- A real-time software simulator (RTSS), implementing the turbine dynamic model and the wind speed model (Burton *et al.,* 2001; Diop *et al.,* 1999; Diop *et al.,* 2007; Nichita, 1995; Nichita *et al.,* 1998 ).

The servo-system is controlled by the RTSS with a torque control loop. The servo-system receives a torque reference and responds by sending back to the RTSS the measured shaft rotational speed. The wind turbine shaft is directly coupled to a Southwest Windpower® Whisper WHI 200 PMSG, having 1 kW rated power. The power limitation of this turbine is ensured by stall control. The torque coefficient, $C_T(\lambda)$, where $\lambda$ is the tip speed ratio of the considered wind turbine has a adopted generic $C_T(\lambda)$ curve parameterised such that the optimal tip speed, $\lambda_{opt}$=7. An important function of the RTSS is the real-time wind speed generation. The subsystem achieving this function can ensure the next distinct regimes:

a – constant speed regime, adjustable in real time through the ControlDesk® interface accompanying the dSPACE board (used in case of Fig.2 and Fig.3 for determining the static characteristics);

b – turbulent wind regime, where the average wind speed is adjustable in real time through the ControlDesk® interface. The wind speed turbulence component depends of the current average wind speed and is obtained with a second-order rational shaping filter by imposing a desired value of the turbulence intensity, $I_t$:

$$(1)\ I_t = \sigma_t / \overline{v}$$

where $\sigma_t$ is the standard deviation of the turbulence component and $\overline{v}$ is the average wind speed. The turbulence intensity is established upon von Karman's or Kaimal's expressions of the spectral density function by using computation relations according to some usual standards: IEC 1400-1, Danish standard DS 472, *etc*. These relations have as parameters the ground surface roughness and the height from the ground (Diop *et al.,* 2007; Nichita, *et al.,* 2002).

The transfer function of the rational shaping filter using von Karman's model of turbulence is:

$$(2)\ H_t(s) = K_F \cdot \frac{m_1 T_F s + 1}{(T_F s + 1)(m_2 T_F s + 1)}$$

where $m_1 = 0.4$, $m_2 = 0.25$ and turbulence parameters $K_F$ and $T_F$ are computed in function of the average wind speed (Diop *et al.,* 2007; Nichita, *et al.,* 2002 ).

The experimental rig's structure has a load adaptation circuit in order to ensure operation of the turbine on the ORC regime. The load adaptation circuit, coupled at the PMSG output, is composed of a rectifier and a chopper embedded in the power optimal control loop (Fig.1).

The wind turbine characteristics implemented in the RTSS are: the blade length, R, is 1.15m, the adopted torque coefficient, $C_T(\lambda)$, curve was parameterized such as the optimal tip speed ratio value is $\lambda_{opt}$ = 7 and the optimal value for power coefficient is $C_{Popt}$=0.476. From Fig.2 it can be seen that the maximum power is obtained for $\lambda$ = 7, so this is the optimal value for the tip speed ratio. The adopted torque coefficient curve is modelled as a $6^{th}$-order polynomial function:

$$(3)\ \begin{aligned} C_T(\lambda) &= a_6\lambda^6 + a_5\lambda^5 + a_4\lambda^4 + \\ &a_3\lambda^3 + a_2\lambda^2 + a_1\lambda + a_0 \end{aligned}$$

where the $a_i, i = \overline{0,6}$ coefficients were determined through polynomial regression starting from the real torque characteristic.

With K2 closed (Fig.1), tests were made and in Fig.2 and Fig.3 are presented some static characteristics. Experimental values are with circle (o). Also the ORC of the analyzed wind system is presented in Fig.3.

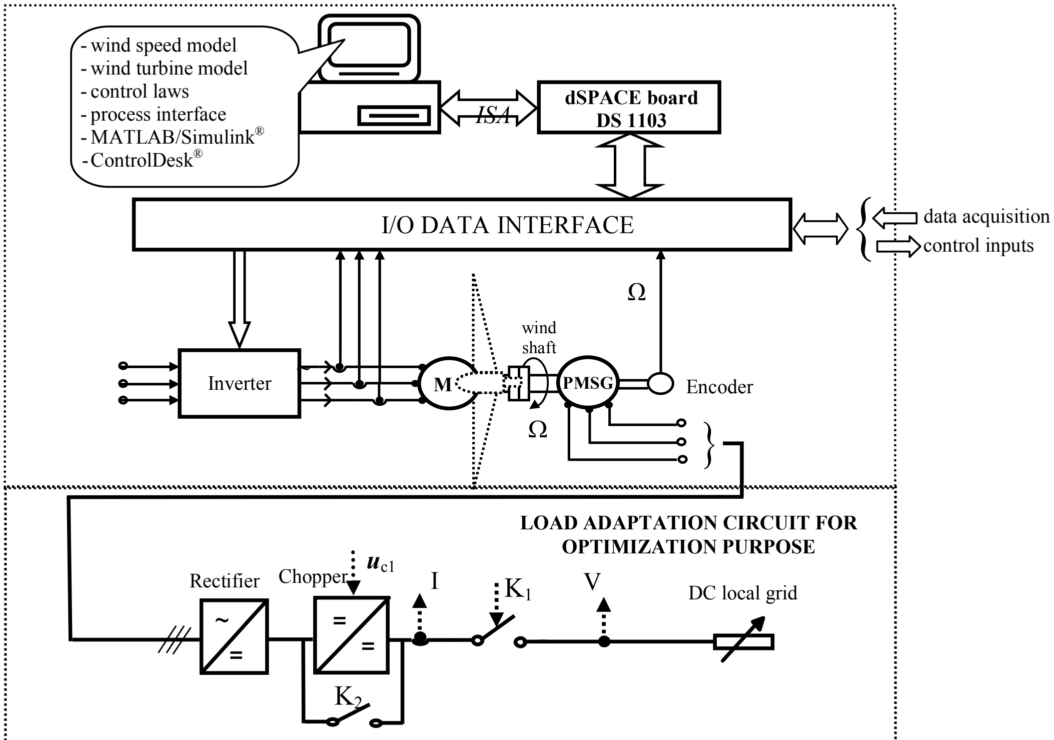


Fig.1. Block diagram of the experimental rig

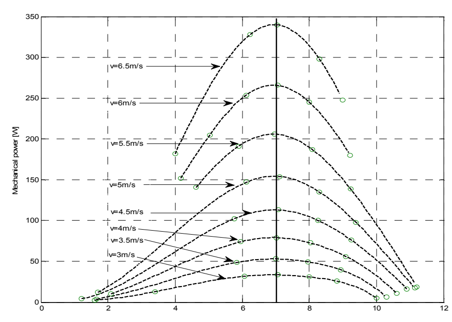


Fig.2. Mechanical power versus tip speed ratio

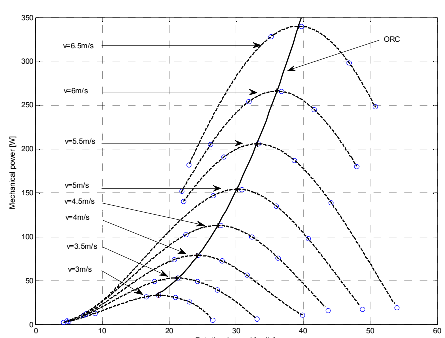


Fig.3. Mechanical power versus wind shaft rotational speed

## 3. PI SPEED CLOSE LOOP CONTROL SOLUTION

The servo-system is controlled by the RTSS in a torque control loop; the servo-system receives a torque reference and responds by sending back to the RTSS the measured shaft rotational speed.
The aerodynamic power is:

$$P_{wind} = \frac{1}{2} \cdot C_p(\lambda) \cdot \rho \cdot \pi \cdot R^2 \cdot v^2 = \frac{1}{2} \cdot \frac{C_p(\lambda)}{\lambda^3} \cdot \rho \cdot \pi \cdot R \cdot \Omega_t^3 \quad (4)$$

where $C_p(\lambda)$ – power efficiency coefficient of the turbine; $\rho$ - air density [kg/m$^3$]; $R$ – rotor blade length [m]; $v$ – single point wind speed in the axial direction [m/s]; $\lambda$ – tip speed ratio:

$$\lambda = \frac{\Omega_t \cdot R}{v} \quad (5)$$

with $\Omega_t$ - rotational speed of wind turbine.
The mechanical rotor torque ($T_{wind}$) is given by:

$$T_{wind} = \frac{P_{wind}}{\Omega_t} \quad (6)$$

By replacing the maximum/optimal values of $\lambda(t) = \lambda_{opt}$ and $C_p = C_p\left(\lambda_{opt}\right)$, one obtains the power reference:

$$(7)\ P_{wind_{opt}} = K \cdot \Omega_{t_{opt}}^3$$

where:

$$(8)\ K = \frac{1}{2} \cdot \frac{C_p\left(\lambda_{opt}\right)}{\lambda_{opt}^3} \rho \pi R^5$$

Equivalently, the wind torque must be equal the optimal value

$$(9)\ T_{wind_{opt}} = K \cdot \Omega_t^2$$

with $K$ defined by relation (8).

The shaft rotational speed optimal control solution using a set point from the wind speed information can be applied if the optimal value of the tip speed ratio, $\lambda_{opt}$, is known. The turbine operates on the ORC if $\lambda(t) = \lambda_{opt}$, which supposes that the shaft rotational speed is closed-loop controlled such that to reach its optimal value:

$$(10)\ \Omega_{t_{opt}}(t) = \frac{\lambda_{opt}}{R} \cdot v(t)$$

So, if the tip speed ratio and the power coefficient have the optimal values, also the shaft rotational speed is optimal. If these three parameters have optimal values, also the wind power has the maximum value. See relations (7) and (8).

Three situations are analysed for the control algorithms which aim to maximize the wind power by keeping the shaft rotational speed at the optimal value:

- a) the anemometer is in front of the wind turbine blades (see Fig.4);
- b) the anemometer is in the back of the wind turbine blades;
- c) there is no anemometer; case used in simulation studies, the wind speed is one meet on the blade surface.

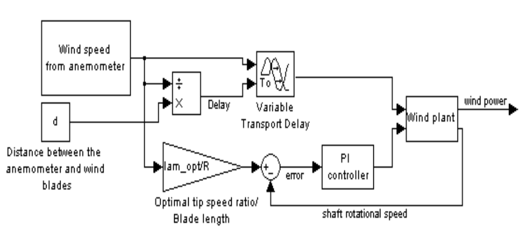


Fig.4. Speed control loop with anemometer in front of the wind turbine blades

## 4. RESULTS

The used wind speed profile with mean value, Vm=6m/s, is showed in Fig.5. Further, for the analyzed situations, the main parameters evolutions: power coefficient, tip speed ratio and optimal regimes characteristic, are presented. Comparing the results from Fig.6, 7 and 8 one can see that small variations of power coefficient are obtained when the anemometer is situated in front of the wind blades at 1 meter. The same results are obtained for tip speed variations (Fig.9 and 10).

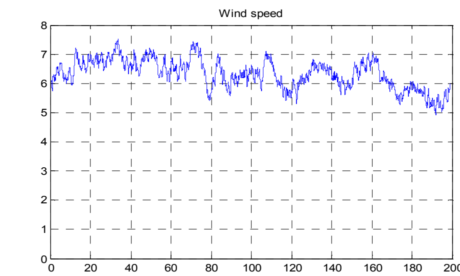


Fig.5. Wind speed profile

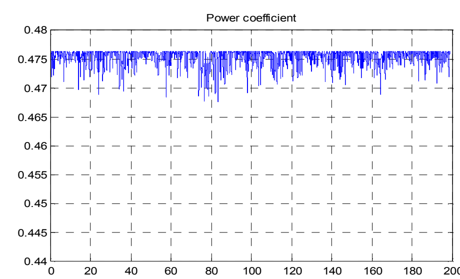


Fig.6. Power coefficient variation -situation a)

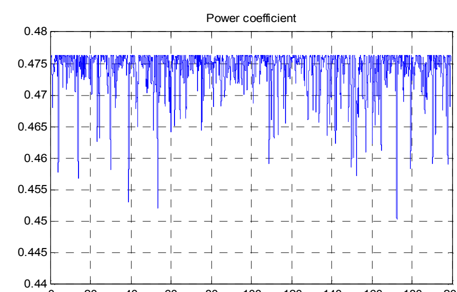


Fig.7. Power coefficient variation -situation b)

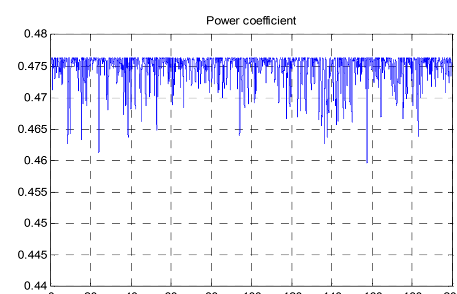


Fig.8. Power coefficient variation -situation c)

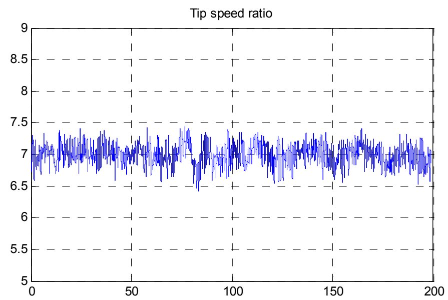


Fig.9. Tip speed ratio variation -situation a)

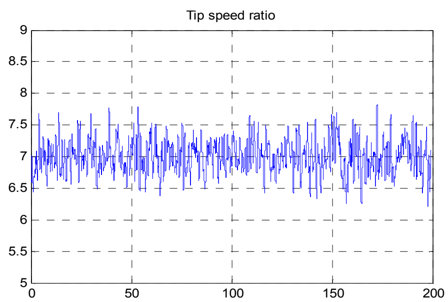


Fig.10. Tip speed ratio variation -situation b)

In Fig.11 and Fig.12 are presented ORC evolutions. When the anemometer is in back of the wind turbine's blades can be seen larger deviations of ORC compared with ones when the anemometer is in front of the blades. To improve the results from situation b) a predictor must be used.

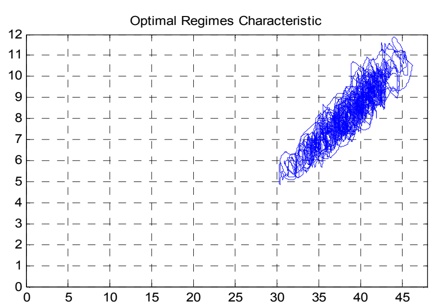


Fig.11. ORC -situation a)

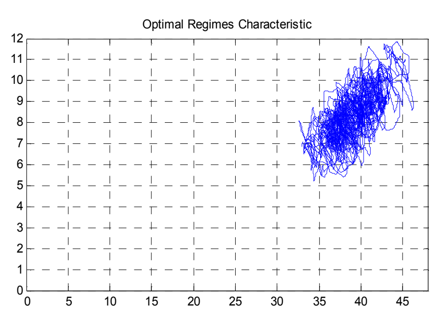


Fig.12. ORC -situation b)

Analyzing the results from Fig.6 to Fig.10 can be said that the system responses depend of the delay between two speed measurements. The wind from anemometer is not the same with one wich act on wind turbine's blades. Also, the dynamic of the wind system must be compensated. A improvement is obtained when the delay of *"Variable Transport Delay"* block from Figure 4 compensate the air mass propagation time from anemometer to wind turbine's blades.

## 5. CONCLUSIONS

This paper has approached the problem of maximization of wind power using shaft rotational speed close loop. The shaft rotational speed optimal control approach using a set point from the wind speed information has some drawbacks related to the wind speed being measured by an anemometer mounted on the nacelle, which offers information on the fixed-point wind speed. A solution was proposed to improve the MPPT algorithm when data for the wind speed anemometer are used as presented above. Comparing the situation when the optimization loop reference is calculated directly from wind anemometer output an improvement was obtained with the proposed method as can be seen from the real-time obtained results.

## 6. REFERENCES

Alatalo, M. (1996). Permanent magnet machines with air gap windings and integrated teeth windings. Technical Report 288, Chalmers University of Technology.

Burton, T., D. Sharpe, N. Jenkins and E. Bossanyi, 2001. *Wind Energy Handbook*, John Wiley & Sons.

Diop, A.D., Nichita, C., Belhache, J.J. Dakyo, B. Ceangă, E., 1999. Modelling variable pitch HAWT characteristics for a real time wind turbine simulator, *Wind Engineering*, Vol.23, No.4, pp. 225-243.

Diop, A.D., Ceangă, E., Rétiveau, J.L., Méthot, J.F., Ilinca, A., 2007. Real-time three-dimensional wind simulation for windmill rig tests, *Renewable Energy*, Vol.32, No.13, pp. 2268-2290.

Munteanu, I., Bratcu, A.I., Cutululis, N.A., Ceangă, E., 2008. Optimal Control of Wind Energy Systems – Towards a Global Approach, Springer-Verlag London.

Nichita C., 1995. Étude et développement de structures et lois de commande numériques pour la réalisation d'un simulateur de turbine éolienne de 3 kW. Ph.D. Thesis, Université du Havre.

Nichita, C., Diop, A.D, Belhache, J.J, Dakyo, B., Protin, L., 1998. Control structures analysis for a real time wind system simulator, *Wind Engineering*, Vol.22, No.6, pp. 275-286.

Nichita, C., Luca, D., Dakyo, B., Ceangă, E., 2002. Large band simulation of the wind speed for real time wind turbine simulators, *IEEE Transactions on Energy Conversion*, Vol.17, No.4, pp. 523-529.

Tan, K., Islam, S., 2004. Optimum control strategies in energy conversion of PMSG wind turbine system without mechanical sensors, *IEEE Transactions on Energy Conversion*, Vol.19, No.2, pp. 392-399.

Vlad, C., 2008. Contribuţii privind modelarea şi analiza experimentală a dinamicii sistemelor autonome eoliene, doctoral report, Galati.